



# Influence of acetate and formate-based deicers on ASR in airfield concrete pavements

Colin Giebson<sup>\*</sup>, Katrin Seyfarth, Jochen Stark

F.A. Finger-Institute for Building Materials Science, Department of Civil Engineering, Bauhaus-University Weimar, Germany

## ARTICLE INFO

### Article history:

Received 31 October 2008

Accepted 10 September 2009

### Keywords:

Alkali–silica reaction

Airfield concrete pavement

Airfield deicer

Thermodynamic calculation

Performance test

## ABSTRACT

In the past few years, the issue of external alkalis and their influence on ASR in concrete has become more important since several concrete airfield pavements have shown ASR-distress related to the use of alkali-containing airfield deicers based on acetates and formates.

Experiments with model pore solutions and cement pastes as well as speciation calculations and ASR performance tests were conducted to investigate possible mechanisms. The obtained results indicate that the solubility of portlandite is increased in the presence of acetate-based and formate-based deicers due to the formation of Ca-acetate and Ca-formate complexes. The additional release of OH<sup>−</sup> ions from portlandite and the supply of alkalis can initiate and highly accelerate ASR in concretes with reactive aggregates. There is also evidence for a reaction of ettringite with such airfield deicers.

© 2009 Elsevier Ltd. All rights reserved.

## 1. Introduction

It has been suspected, that the action of alkali-containing deicers is capable of favoring an alkali–silica reaction (ASR) in concrete with reactive aggregates. The research in the past decades was mainly focused on the effects of sodium chloride [1,2]. For safety reasons, chloride-based deicers are not used on airfields in order to avoid corrosive damage to aircraft and airport equipment. Therefore, synthetic urea (CH<sub>4</sub>N<sub>2</sub>O) and certain alcohols, e.g. ethylene glycol (C<sub>2</sub>H<sub>6</sub>O<sub>2</sub>), have been used as airfield deicers. Deicers based on sodium and potassium acetate (CH<sub>3</sub>COOK) and later based on sodium and potassium formate (HCOOK), were introduced in the United States of America as well as in Germany in the early 1990s. These deicing chemicals possess several advantages over traditional deicing chemicals. They are more environmentally friendly, since they are readily biodegradable, leaving behind only harmless, non-toxic residues and contain no nitrogen. They are also more effective at lower temperatures, work faster and longer and require fewer applications. Acetate-based deicers have also been used for highway and bridge deck anti-icing efforts, to take advantage of the environmental benefits and prevent reinforced concrete structures from chloride-induced corrosion damage.

However, in the past few years severe ASR-distress has been observed in concrete airfield pavements with increasing frequency. It was reported that about thirty U.S. military airfields around the world and at least eight commercial U.S. airports have been affected by an

increase in ASR-induced damage. Even concrete mixtures with low-alkali cements have suffered deleterious ASR. The damages (map-cracking, aggregate pop-out, buckling/heaving) not only cause expensive repairs but possibly also pose an increased foreign object damage (FOD) hazard to aircraft [3–6]. At the FIB (F.A. Finger-Institut für Baustoffkunde), a German runway was investigated in the late 1990s that showed ASR-induced damages nearly 7 years after the deicer was changed from urea to potassium acetate. At that time it was already supposed that there is a relation between the damages and the application of the potassium acetate deicer.

Commercial deicer solutions contain about 50–55% active components and minor amounts of corrosion inhibitors. To improve the effectiveness, solid deicers (sodium-based) and liquid deicers (potassium-based) are often used in combination. The application rates depend strongly on the weather situation and are usually about 10–60 g/m<sup>2</sup>. The deicers are either applied to melt accumulated layers of snow and ice on the pavement surface (deicing) or they are applied prior to an expected precipitation event on the bare pavement surface (anti-icing) to prevent the accumulation of snow and ice. In Germany, there are approximately 40–50 days of deicing/anti-icing within every winter period with several applications per day if necessary. So far, only a few studies are available that investigated the influence of these deicers on ASR in concrete.

Since 2001, an alternating climate test method (cyclic climate storage) has been used at the FIB for accelerated simulation of Central European climatic conditions, in order to assess the durability of project-specific concretes for outdoor structures. Significant factors from environmental effects (wetting and drying, freezing and thawing and exposure to deicing chemicals) are simulated to observe degradation characteristics of the concrete under test by alternating temperature and moisture conditions in a special developed climate simulation chamber. More than one hundred fifty concretes comprised

<sup>\*</sup> Corresponding author.

E-mail address: [colin.giebson@uni-weimar.de](mailto:colin.giebson@uni-weimar.de) (C. Giebson).

mainly of field representative concrete with different cement types and most containing slow/late alkali–silica reactive aggregates have been tested in the aforementioned conditions. The results clearly showed that deleterious ASR can be initiated and accelerated in concretes with reactive aggregates exposed to alkali-containing deicers, especially based on acetates and formates (Fig. 1). In this case, even low-alkali cements are not capable of permanently preventing deleterious ASR [7–9]. To provide an explanation for these observations, investigations into the mechanisms were performed and are introduced below.

## 2. Materials and methods

### 2.1. Materials and sample preparation

#### 2.1.1. Solubility experiments

Solubility experiments were performed using pure powders of  $\text{Ca}(\text{OH})_2$  (portlandite),  $\text{CH}_3\text{COOK}$  (K-acetate),  $\text{HCOOK}$  (K-formate),  $\text{Ca}(\text{CH}_3\text{COO})_2$  (Ca-diacetate) and  $\text{CaSO}_4 \cdot 2\text{H}_2\text{O}$  (gypsum) for comparison purposes. The water used was double distilled and boiled to remove dissolved carbon dioxide. The deicing chemicals were mixed in different concentrations (0.05, 0.3, 1.5 and 2.5 mol/l) into saturated solutions (200 ml) of portlandite with solid portlandite in excess. Compared to commercial deicers, lower concentrations of the deicing chemicals were chosen for these experiments to consider the limitations of the used approach for the calculation of the species distribution in the solutions. The experiments were done in a glove-box, using nitrogen as the inert gas to avoid any possible degradation of the deicing chemicals with the presence of oxygen and to avoid precipitation of calcium carbonate. K-acetate (0.05, 0.3, 1.5 and 2.5 mol/l) was also mixed in a saturated solution (200 ml) of gypsum with solid gypsum in excess. All solutions were sealed in airtight plastic vials and stored for 24 h at 20 °C. The solutions were analyzed by ICP-OES and the pH was measured by using an alkali-resistant glass electrode (Orion ROSS, 81-08). Selected solid residues were filtered, dried at 40 °C and analyzed by XRD, FT-IR and ESEM/EDS.

#### 2.1.2. Cement paste experiments

Cement pastes were made from two portland cements with different  $\text{Na}_2\text{O}_{\text{eq}}$  (0.44 and 0.81 wt.%) and a w/c of 0.42. After 7 days of curing in airtight sealed vials at 20 °C, the hardened samples ( $\varnothing$  30 mm,  $l$  = 30 mm) were vacuum-immersed in two commercial airfield deicer solutions (K-acetate and K-formate) and in water respectively. The vacuum immersion was done 5-times in series of decompression (15 min) and compression. After the vacuum immersion, the samples were sealed airtight in a polyethylene bag and stored at 40 °C for 14 days. Afterwards, the pore solution was

expressed and analyzed by ICP-OES. Additional cement paste samples were examined by XRD and ESEM/EDS. The entire procedure with the three steps of vacuum immersion, storage at 40 °C for 14 days and the subsequent analysis of the samples was repeated 5-times up to a sample age of 77 days.

#### 2.1.3. ASR performance tests

Three concrete mixtures representative of airfield concrete were tested with the FIB cyclic climate storage as an ASR performance test to assess the potential for deleterious ASR if exposed to a commercial K-acetate deicer solution. All mixtures contained the same reactive greywacke aggregate (2–22 mm) and a non-reactive quartz sand (0–2 mm), but for every mixture a portland cement with different  $\text{Na}_2\text{O}_{\text{eq}}$  (0.54, 0.68 and 0.90 wt.%) was used. In every case, the portland cement content was 370 kg/m<sup>3</sup> without added alkalis (unboosted), the w/c ratio was 0.42 and all concrete mixtures were air-entrained and contained 4.6–4.7% air. Concrete prisms (100 × 100 × 400 mm) were cast from each mixture with embedded stainless steel studs cast in each end for expansion measurements. After 24 h, the prisms were demolded, wrapped airtight in polyethylene foil and stored for 5 days at 20 °C. Subsequently, a flexible foam rubber tape was glued around the upper edges of the prisms to form a guard that will retain the applied test solution. The cyclic climate storage was initiated 7 days after casting. A commercial K-acetate deicer solution was placed on top of three prisms from each mixture. The deicer solution was diluted to 0.6 mol/l prior to the application of 400 g on each of the three prisms. Concentration and application amounts were chosen based on preliminary studies to ensure conditions that are comparable to the field. With some assumptions, the amount of the commercial deicer solution that is applied with every cycle (1200 g/m<sup>2</sup>) corresponds nearly to the average amount that is applied during one winter period in the field on runways of German international airports. A set of three prisms from each mixture were treated with distilled water as the control. The cyclic climate storage was done for 16 cycles or 12 months respectively. After the cyclic climate storage thin sections were examined and investigations with ESEM/EDS were performed.

### 2.2. Methods for assessment and analysis

#### 2.2.1. Inductively coupled plasma-optical emission spectrometry (ICP-OES)

About 20 ml of the solutions from the solubility experiments and 2–5 ml of the expressed pore solutions were filtered (0.45 µm) and sealed airtight in plastic vials. The solutions were diluted (1:100) with nitric acid (1%) and about 100 µl was injected in the argon-plasma of the spectrometer (Perkin-Elmer, Optima 3000). The element concentrations of K, Na, Ca and S were determined. The detection limits ranged from 0.02 µg/l (Ca) to 30 µg/l (S).

#### 2.2.2. X-ray powder diffraction (XRD)

Solid residues were prepared in the glove-box by separation from the solution with a frit (40 µm) and then rinsed with isopropanol and acetone. The residue was applied on a polyethylene sample holder, covered with a sheet of polypropylene and then discharged from the glove-box. The cement paste samples were crushed by hand with hammer and chisel and further reduced gently with a corundum mortar and pestle to obtain a coarse powder. The powder was rinsed with isopropanol and acetone in order to stop hydration. After the grinding phase, the powder was dried for 30 min at 40 °C prior to gently grinding by hand with a mortar and pestle of corundum until all particles passed the 40 µm sieve. About 2 g of the fine powder was placed in a polyethylene sample holder. The X-ray diffractometer (Siemens, D-5000) operates with  $\text{Cu-K}_\alpha$  radiation with a wavelength  $\lambda$  of 0.154 nm. Diffractograms were recorded from 4 to 60° 2 $\theta$ , in 0.05° 2 $\theta$  increments with 2.5 s counting time per increment.

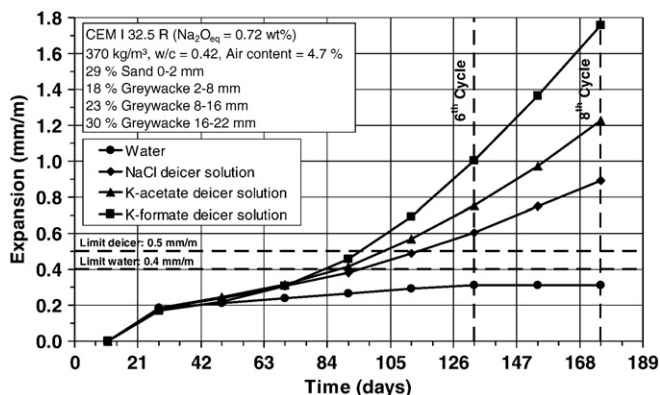


Fig. 1. Expansion during the cyclic climate storage for a tested pavement concrete with reactive greywacke aggregates, exposed to different deicer solutions and water (control).

**Table 1**  
Supplementary thermodynamic data for speciation calculations at 25 °C.

Phases and species	Formula	Reaction	log $K^a$	Reference
Portlandite	$\text{Ca}(\text{OH})_2$ (s)	$\text{Ca}^{2+} + 2 \text{OH}^-$	−5.19	[10]
Acetic acid	$\text{CH}_3\text{COOH}$ (aq)	$\text{H}^+ + \text{CH}_3\text{COO}^-$	−4.76	[16]
Potassium acetate	$\text{CH}_3\text{COOK}$ (aq)	$\text{K}^+ + \text{CH}_3\text{COO}^-$	+0.34	[16,21]
Calcium monoacetate	$\text{CaCH}_3\text{COO}^+$ (aq)	$\text{Ca}^{2+} + \text{CH}_3\text{COO}^-$	−0.85	[16,21]
Calcium diacetate	$\text{Ca}(\text{CH}_3\text{COO})_2$ (aq)	$\text{Ca}^{2+} + 2 \text{CH}_3\text{COO}^-$	−1.25	[16,21]
Formic acid	$\text{HCOOH}$ (aq)	$\text{H}^+ + \text{HCOO}^-$	−3.75	[16]
Potassium formate	$\text{HCOOK}$ (aq)	$\text{K}^+ + \text{HCOO}^-$	−0.03	[16,22]
Calcium monoformate	$\text{CaHCOO}^+$ (aq)	$\text{Ca}^{2+} + \text{HCOO}^-$	−1.40	[16,22]
Calcium diformate	$\text{Ca}(\text{HCOO})_2$ (aq)	$\text{Ca}^{2+} + 2 \text{HCOO}^-$	−2.24	[16,22]

<sup>a</sup> Calculated by using  $\Delta_r G^\circ = -RT \ln K$  with data from the given reference.

### 2.2.3. Fourier-transform infrared spectroscopy (FT-IR)

Solid residues were prepared in the glove-box by separation from the solution with a frit (40 µm) and rinsed with isopropanol and acetone. Then, the residues were dried for 30 min at 40 °C and used as obtained for the analysis. Solutions were filtered (40 µm) and sealed in an airtight plastic vial. The samples were placed into the spectrometer (BioRad, FTS 175L) and the absorbance was determined from 400 to 4000  $\text{cm}^{-1}$ . For these solutions, a pure water sample was recorded and subtracted from the sample spectra.

### 2.2.4. Environmental scanning electron microscopy with energy-dispersive X-ray spectroscopy (ESEM/EDS)

An environmental scanning electron microscope (Philips, XL 30 ESEM-FEG) equipped with an EDS-detector was used to examine single phases and to determine their composition. Since samples did not need to be coated, they were studied in situ without artifacts. Operating conditions were set to 25–10 kV and 10–3 Torr. Immediately before the ESEM/EDS analysis, the samples were obtained from the core of the cement paste samples and from the concrete prisms respectively by creating a freshly fractured surface with hammer and chisel and without any further preparation.

### 2.2.5. Speciation calculation with PHREEQC

Speciation calculations were performed using PHREEQC [10] to explain experimental results and to predict possible mechanisms. The WATEQF4-database and the supplementary reactions given in Table 1 were used for the modeling. In order to account the interactions in aqueous solutions, the activities were calculated with activity coefficients obtained from the Davies equation, which is based on the ion-association approach according to Debye–Hückel. This approach will become unreliable with increasing ionic strength (already >0.5 mol/l), so that the ion-interaction approach according to Pitzer should be used for the solutions with a high ionic strength tested in this research. However, the required parameters for the ion–ion interactions of interest were not available in the known literature.

### 2.2.6. ASR performance-testing with the FIB cyclic climate storage

In a special walk-in climate simulation chamber (Feutron, Type 3705/04), the prepared concrete prisms were stored under a pre-defined cycle of alternating temperature and moisture conditions [7,8,11–15]. One cycle lasts 21 days and consists of 4 days of drying at 60 °C and ≤10% relative humidity (RH), 14 days of wetting at 45 °C and 100% RH and 3 days of freeze–thaw-cycling between +20 °C and −20 °C (Fig. 2). At the end of the first drying phase the initial length and mass are measured and 400 g of the test solution (deicer or water respectively) is applied to every prism for the first time and this solution remains on the prisms until the end of the cycle. After the cycle, the test solution is removed to measure length change and mass of the prisms and is replaced once the readings were taken. All measurements were done at 20 °C. During the second drying phase, the water of the test solution evaporates, leaving behind minor solid residues from the deicer as well as leached substances from the

concrete, e.g. alkalis, sulfate etc. At the end of the second drying phase new test solution is applied. For this investigation the cyclic climate storage continued for 16 cycles (12 months) to illustrate basic trends more clearly. For pavement concretes exposed to deicers it was found that 8 cycles (6 months) are usually sufficient to assess the potential regarding deleterious ASR correctly, compared to the typical period after which ASR-damages appear in the field on concretes with slow/late reacting aggregates [14,15]. The expansion limits were defined as 0.5 mm/m for application of deicer solutions (higher moisture impact) and as 0.4 mm/m for application of water only. Additionally, the slope of the expansion curve between 6 and 8 cycles was evaluated and microscopic examinations were performed after the cyclic climate storage was finished.

### 2.2.7. Thin section analysis

After the cyclic climate storage, one thin section (6×10 cm) was prepared from a prism of each mixture exposed to deicer solution and water respectively. The samples were cut from the middle of the prisms. The longer side (10 cm) represents the full height of the prism. Pores and cracks were filled by vacuum impregnation with a special yellow colored resin. The thin sections were investigated under an optical polarizing microscope (Zeiss, Jenalab).

## 3. Results

### 3.1. Solubility experiments

The initial pH of the saturated  $\text{Ca}(\text{OH})_2$  solutions immediately increased after addition of  $\text{CH}_3\text{COOK}$  or  $\text{HCOOK}$ . Analysis of the resulting solutions by ICP-OES furthermore revealed an increased Ca concentration (Fig. 3). The difference between the measured (12.31) and the calculated pH (12.46) of the saturated  $\text{Ca}(\text{OH})_2$  solution without deicer is probably caused by inaccuracies during the measurement or because the equilibrium was not yet approached. The results of the XRD, FT-IR

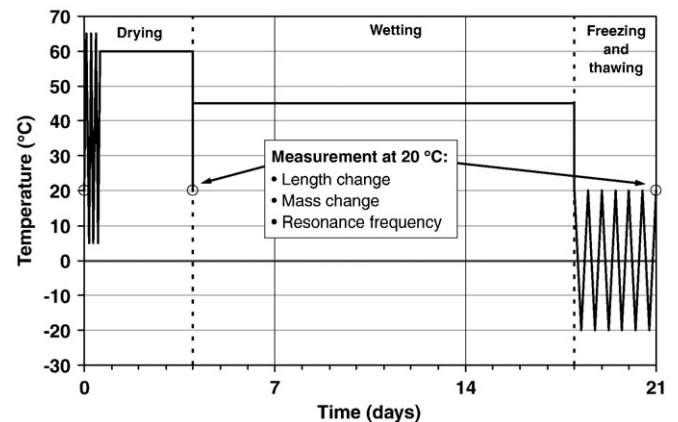


Fig. 2. Temperature scheme for one cycle of the cyclic climate storage.

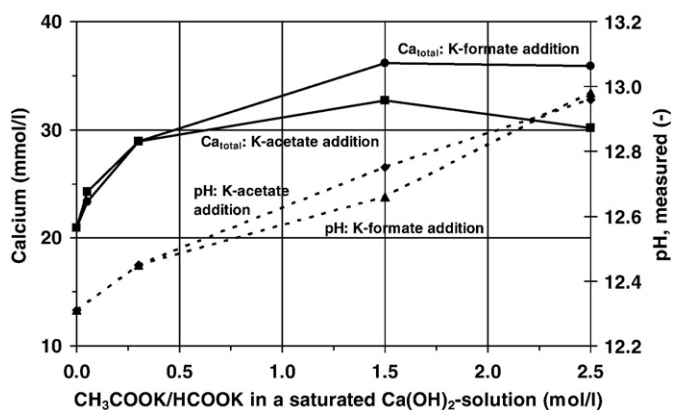


Fig. 3. Increase of pH and Ca concentration in a saturated solution of Ca(OH)<sub>2</sub> with addition of CH<sub>3</sub>COOK and HCOOK respectively.

and ESEM/EDS analysis showed no new precipitation products in the solid residues. The FT-IR analysis of a saturated Ca(OH)<sub>2</sub> solution with addition of CH<sub>3</sub>COOK (2.5 mol/l) showed the same spectra as a solution of CH<sub>3</sub>COOK (2.5 mol/l) alone. Compared to a solution of Ca(CH<sub>3</sub>COO)<sub>2</sub> (2.5 mol/l), there are only minor differences, mostly in intensity of the typical CH<sub>3</sub>COO<sup>-</sup> bands at 1553 cm<sup>-1</sup> and 1416 cm<sup>-1</sup> (Fig. 4). For comparison, the pH in the saturated solution of CaSO<sub>4</sub>·2H<sub>2</sub>O increased only slightly after addition of CH<sub>3</sub>COOK, but the Ca concentration increased considerably (Fig. 5).

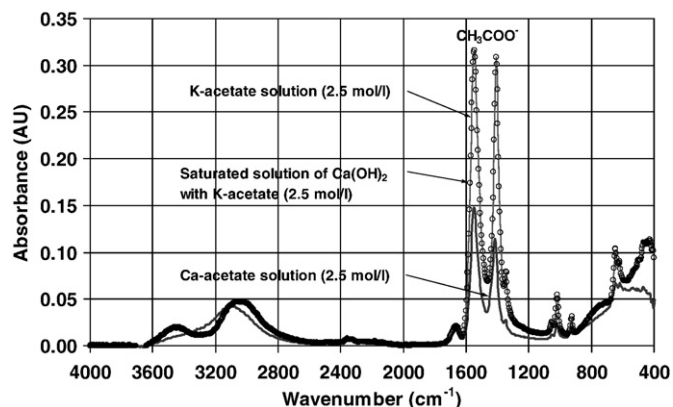


Fig. 4. FT-IR spectra (water subtracted) from solutions (2.5 mol/l) of pure Ca(CH<sub>3</sub>COO)<sub>2</sub>, CH<sub>3</sub>COOK and a saturated solution of Ca(OH)<sub>2</sub> with CH<sub>3</sub>COOK.

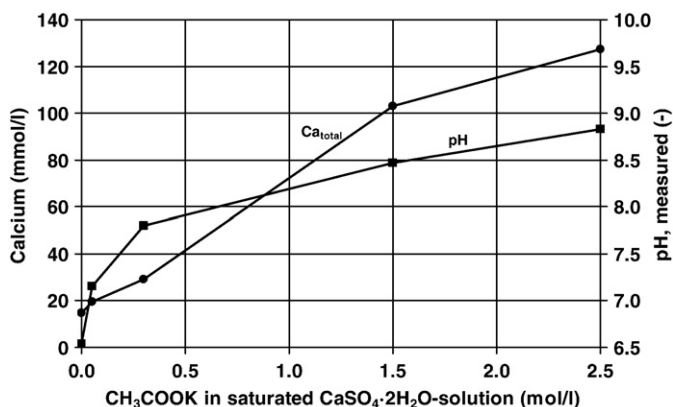


Fig. 5. Increase of pH and Ca concentration in a saturated solution of CaSO<sub>4</sub>·2H<sub>2</sub>O with addition of CH<sub>3</sub>COOK.

For a saturated solution of Ca(OH)<sub>2</sub> with solid Ca(OH)<sub>2</sub> in excess and addition of CH<sub>3</sub>COOK, the speciation calculation shows an increasing pH that is strongly related to the formation of aqueous Ca-acetate complexes (Fig. 6). At low CH<sub>3</sub>COOK concentrations CaCH<sub>3</sub>COO<sup>+</sup> is the dominant complex, at higher concentrations Ca(CH<sub>3</sub>COO)<sub>2</sub> is more stable. Although the concentration of Ca<sup>2+</sup> is decreased, the total Ca concentration in the solution increases. With increasing addition of CH<sub>3</sub>COOK, the increase of pH and the total Ca concentration slow down. Compared to the total CH<sub>3</sub>COO<sup>-</sup> concentration, there are only a few percent of Ca-acetate complexes in the solution. Comparable results were obtained for HCOOK (Fig. 7).

### 3.2. Cement paste experiments

The ICP-OES analysis for the pore solutions of the vacuum-immersed cement paste samples showed an increase of the K concentration for the samples immersed in the deicer solutions (Fig. 8). However, the pH was not affected as much as expected and even decreased for the high-alkali cement pastes (Fig. 9). The Ca concentration and the pH tend to be higher in the cement pastes immersed in the deicer solutions than in water. At later ages (> 35 days), the Ca concentration and the pH increased in the low-alkali cement paste samples immersed in the deicer solutions (Figs. 9 and 10). The SO<sub>4</sub><sup>2-</sup> concentration increased for both cement pastes treated with deicer solution, especially in the case of HCOOK (Fig. 11). The XRD analysis revealed a decrease in the ettringite (3CaO·Al<sub>2</sub>O<sub>3</sub>·3CaSO<sub>4</sub>·32H<sub>2</sub>O) peak for the cement pastes exposed to the deicer solutions.

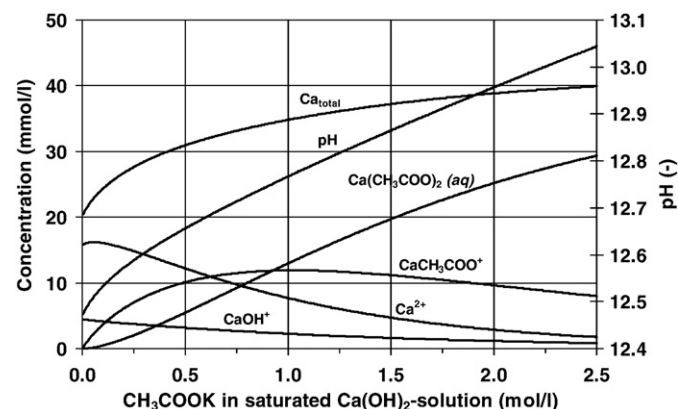


Fig. 6. Calculated species distribution in a saturated solution of Ca(OH)<sub>2</sub> with addition of CH<sub>3</sub>COOK at 25 °C.

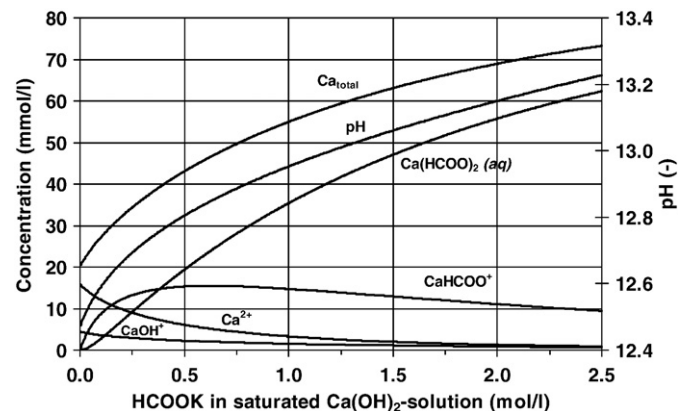


Fig. 7. Calculated species distribution in a saturated solution of Ca(OH)<sub>2</sub> with addition of HCOOK at 25 °C.

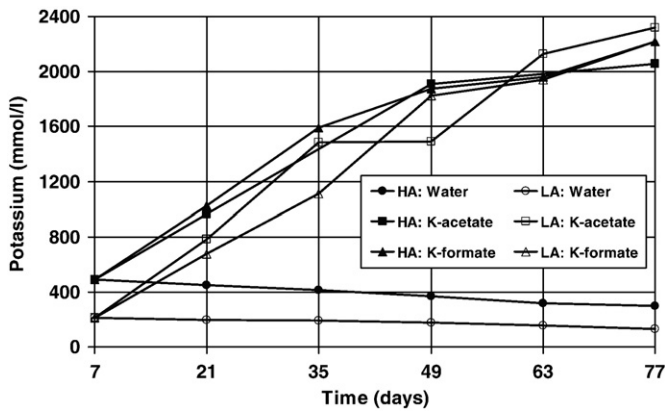


Fig. 8. Pore solution analysis (potassium) for cement paste samples (HA = high-alkali cement, LA = low-alkali cement) treated with two commercial deicer solutions and water respectively.

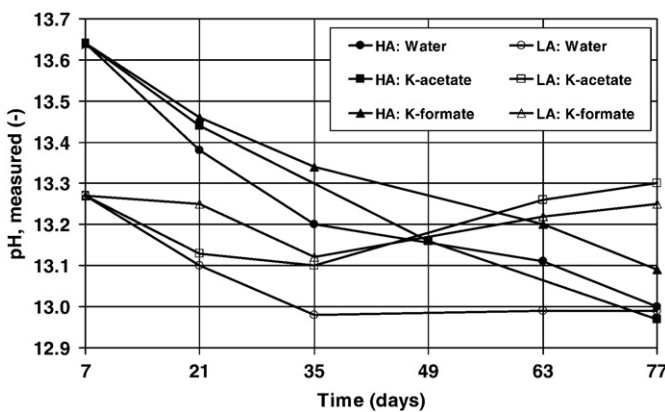


Fig. 9. Pore solution analysis (pH) for cement paste samples (HA = high-alkali cement, LA = low-alkali cement) treated with two commercial deicer solutions and water respectively.

### 3.3. ASR performance tests

The concrete with the high-alkali portland cement ( $\text{Na}_2\text{O}_{\text{eq}} = 0.90 \text{ wt.}\%$ ) exposed to the deicer exhibited a rapidly increasing expansion. After 4 cycles (3 months) the expansion exceeded the limit of  $0.5 \text{ mm/m}$  (Fig. 12). Exposed to water, the expansion increased slower but after 4 cycles (3 months) the limit of  $0.4 \text{ mm/m}$  was exceeded (Fig. 13). The concrete with the medium-alkali portland cement ( $\text{Na}_2\text{O}_{\text{eq}} = 0.68 \text{ wt.}\%$ )

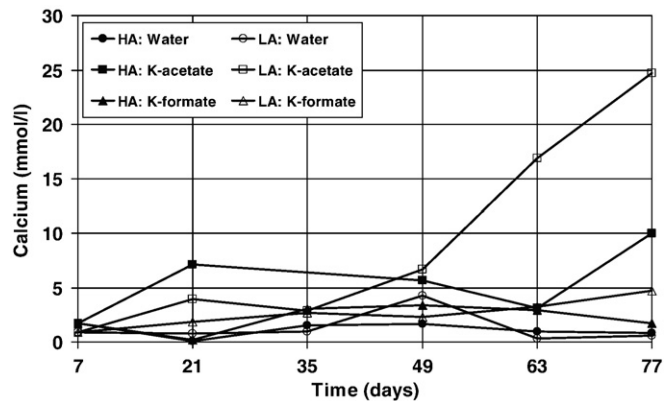


Fig. 10. Pore solution analysis (calcium) for cement paste samples (HA = high-alkali cement, LA = low-alkali cement) treated with two commercial deicer solutions and water respectively.

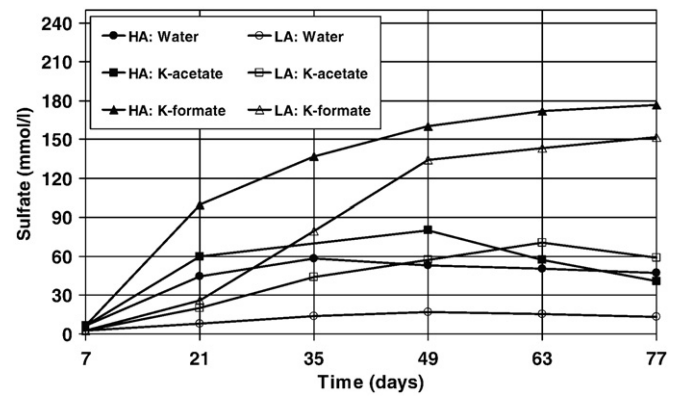


Fig. 11. Pore solution analysis (sulfate) for cement paste samples (HA = high-alkali cement, LA = low-alkali cement) treated with two commercial deicer solutions and water respectively.

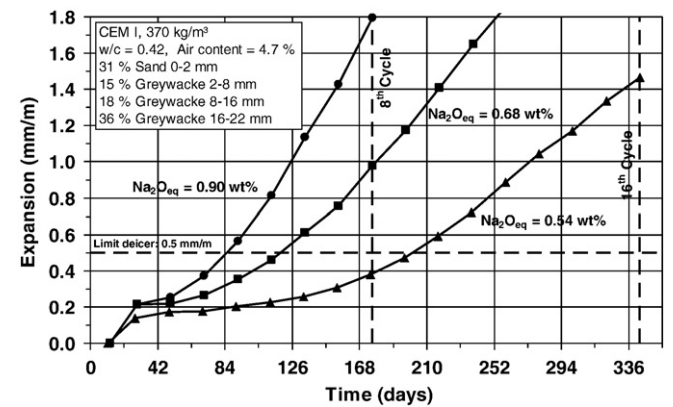


Fig. 12. Expansion during the cyclic climate storage for three tested airfield pavement concretes with reactive greywacke and different cement  $\text{Na}_2\text{O}_{\text{eq}}$  exposed to K-acetate deicer solution.

exposed to the deicer also showed a clearly increasing expansion. After 6 cycles (5 months) the expansion exceeded the limit of  $0.5 \text{ mm/m}$  clearly (Fig. 12). Exposed to water, the expansion increased only slightly and the limit of  $0.4 \text{ mm/m}$  was not exceeded (Fig. 13). For the concrete with the low-alkali portland cement ( $\text{Na}_2\text{O}_{\text{eq}} = 0.54 \text{ wt.}\%$ ) exposed to the deicer (Fig. 12), the expansion increased slowly in the beginning but finally exceeded the limit of  $0.5 \text{ mm/m}$  after 10 cycles (8 months). Exposed to water (Fig. 13), no deleterious expansion occurred in the case of the low-alkali portland cement.

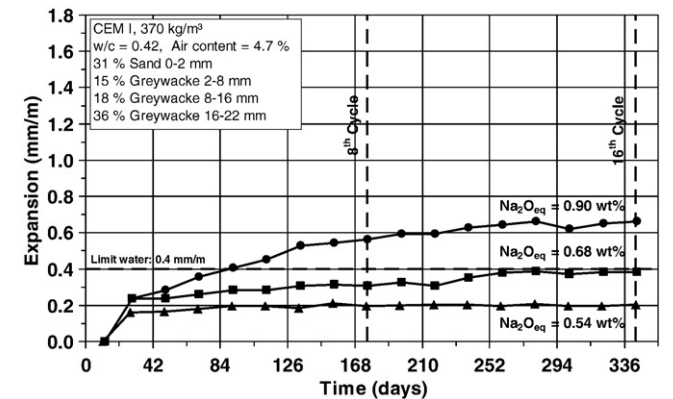
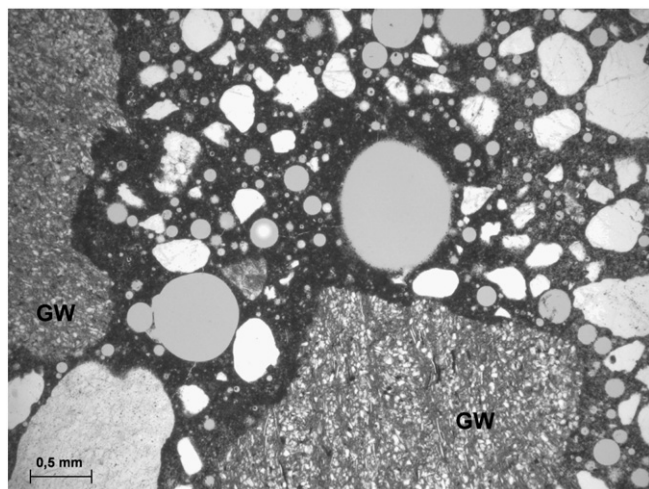
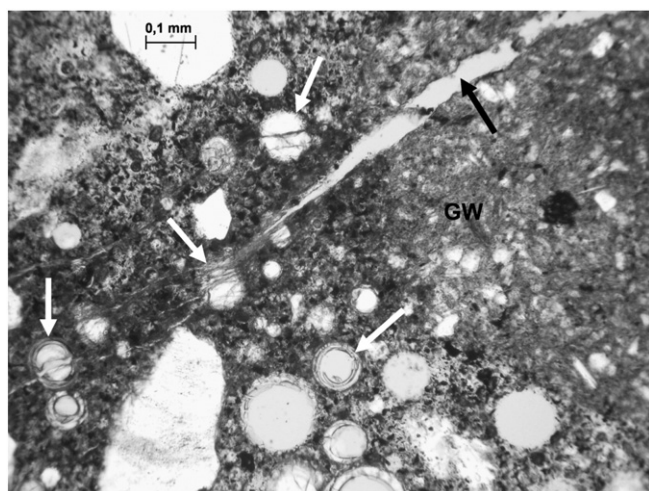


Fig. 13. Expansion during the cyclic climate storage for three tested airfield pavement concretes with reactive greywacke and different cement  $\text{Na}_2\text{O}_{\text{eq}}$  exposed to water.



**Fig. 14.** Thin section image of the low-alkali concrete exposed to water after 16 cycles in the cyclic climate storage shows no evidence for ASR or other damage, GW: sound greywacke grains.



**Fig. 15.** Thin section image of the low-alkali concrete exposed to deicer solution (K-acetate) after 16 cycles in the cyclic climate storage shows clear evidence for deleterious ASR, GW: cracked greywacke grain, the crack (black arrow) propagates in the matrix, ASR-gel infiltrated matrix (darker area), pores with ASR-gel (white arrows etc.).

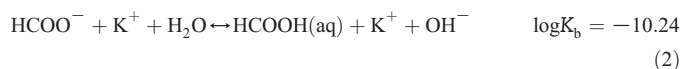
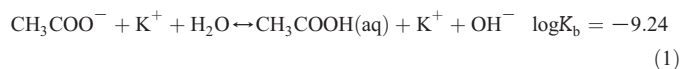
After the cyclic climate storage, micro-cracks were visible to the naked eye on all prisms exposed to the deicer solution but not on the prisms exposed to water. The thin sections showed no evidence for ASR or other damage in the prisms exposed to water (Fig. 14) except for the concrete with the high-alkali portland cement. Clear evidence for deleterious ASR was found in the thin sections of all three concretes exposed to the deicer solution (Fig. 15). This was confirmed by the ESEM/EDS analysis. Frequency and intensity of ASR (gel filled pores and cracks) corresponded to the reached expansion of each mixture. The EDS analysis revealed that the composition of the ASR-gel was clearly influenced by the deicer exposure. The ASR-gel in the prisms exposed to the deicer solution (K-acetate) had a significantly higher potassium content ( $K_2O$ : 8–25 wt.%) than usual ASR-gels as in prisms exposed to water only ( $K_2O$ : 3–10 wt.%).

## 4. Discussion

### 4.1. Solubility experiments

$CH_3COOK$  (2530 g/l at 20 °C) and  $HCOOK$  (3310 g/l at 20 °C) are extremely water-soluble salts of acetic acid ( $CH_3COOH$ ) and formic

acid ( $HCOOH$ ) respectively. Dissolved in water, the acetate and formate ions behave according to the acid–base theory of Brønsted–Lowry as a base and absorb protons from water (Eqs. (1) and (2)). Hence, aqueous solutions of  $CH_3COOK$  and  $HCOOK$  are always slightly alkaline. The pH in such solutions can be calculated by using Eq. (3) and ranges from 9 to 11 for commercial deicer solutions. The smaller the  $pK_b$  value the stronger the base, i.e. the greater its tendency to absorb protons. The equilibrium constants of Eqs. (1) and (2) indicate that only small amounts of the acetate and formate ions form acetic acid and formic acid respectively.



$$pH = 14.0 - 0.5 \cdot (pK_b - \log c) \quad (3)$$

with:

$$pK_b = -\log K_b = \text{basicity constant}$$

$$c = \text{concentration of the acetate/formate ions, [mol/l]}$$

The speciation calculation for the saturated solution of  $Ca(OH)_2$  with addition of  $CH_3COOK$  fits considerably well with the experimental results (Fig. 16). This suggests that the increase of the pH and the total Ca concentration are caused by the formation of aqueous Ca-acetate complexes. For  $HCOOK$ , the mechanism is assumed to be the same, but at higher concentrations there are greater differences between the speciation calculation and experimental results. This could be caused by using an ion-association approach for the calculation of the activity coefficients. With increasing ionic strength, the results will become progressively unreliable due to increasing ion interactions [16]. Furthermore, underlying uncertainties in the thermodynamic data also affect the calculations. Nevertheless, the formation of the Ca-acetate and Ca-formate complexes provides a fundamental explanation for the observed increase of the pH and the total Ca concentration (Eqs. (4)–(7)). Since  $Ca^{2+}$  is consumed for the formation of these complexes, more solid  $Ca(OH)_2$  is dissolved to

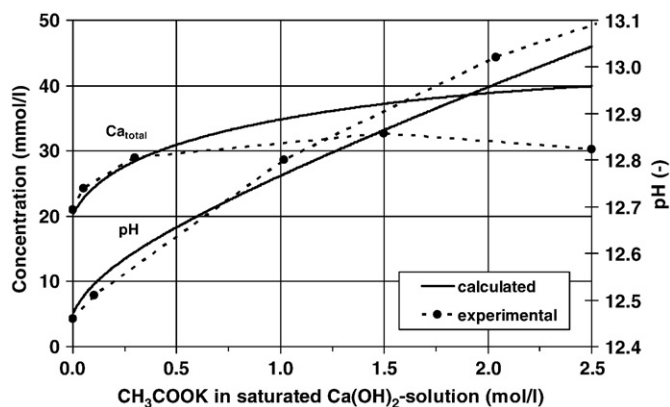
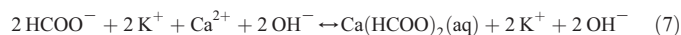
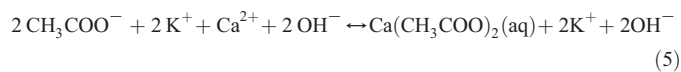
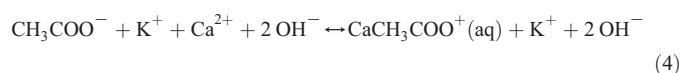


**Fig. 16.** Calculated and measured pH and total Ca concentration in a saturated solution of  $Ca(OH)_2$  with addition of  $CH_3COOK$  at 25 °C.

maintain the equilibrium with the solution (Eq. (8)). Consequently, the pH and the total Ca concentration will increase (Figs. 6 and 7).

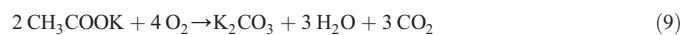


Because of the decreasing solubility of  $\text{Ca}(\text{OH})_2$  with increasing pH, there will be not enough Ca in the solution for a precipitation of solid  $\text{Ca}(\text{CH}_3\text{COO})_2$  and  $\text{Ca}(\text{HCOO})_2$  respectively due to the good solubility of  $\text{Ca}(\text{CH}_3\text{COO})_2$  (300 g/l at 20 °C) and  $\text{Ca}(\text{HCOO})_2$  (160 g/l at 20 °C). That is supported by the findings of the XRD, FT-IR and ESEM/EDS analysis, where no new precipitation products could be found [17]. However, the direct detection of the Ca-complexes turned out to be more difficult. The FT-IR analysis provided no indication for Ca-complexes in the solution on the basis of peak shifts or appearance of new bands (Fig. 4). But the speciation calculation shows that only small amounts of the Ca-complexes are formed, which may aggravate the detection. Furthermore, FT-IR is appropriate to identify organic ions, but not necessarily to which inorganic ions they are linked. An indirect verification provides the increased solubility of  $\text{CaSO}_4 \cdot 2\text{H}_2\text{O}$  in pure water after addition of  $\text{CH}_3\text{COOK}$  (Fig. 5). The solubility of  $\text{CaSO}_4 \cdot 2\text{H}_2\text{O}$  in pure water (2.0 g/l at 20 °C) is comparable to  $\text{Ca}(\text{OH})_2$  (1.7 g/l at 20 °C), but in the  $\text{CH}_3\text{COOK}$  solution (2.5 mol/l), the solubility of  $\text{CaSO}_4 \cdot 2\text{H}_2\text{O}$  increased about 9-times (21.9 g/l at 20 °C). The reason for this is again the formation of aqueous Ca-acetate complexes. Contrary to  $\text{Ca}(\text{OH})_2$ , a much higher Ca concentration is reached, because  $\text{CaSO}_4 \cdot 2\text{H}_2\text{O}$  cannot release  $\text{OH}^-$  ions and consequently no  $\text{Ca}(\text{OH})_2$  will precipitate. The slight increase of the pH is only caused by the deprotonation of water according to Eq. (1).

In a study by Diamond et al., even a pH of 15.1 was measured after addition of  $\text{Ca}(\text{OH})_2$  in a  $\text{CH}_3\text{COOK}$  solution of 50 wt.%, which is a typical concentration (6.2 mol/l) of commercial airfield deicer solutions [18]. The existence of Ca-acetate complexes was confirmed in the study by Frantz using Raman-spectroscopy [19]. It was found that in Ca-acetate solutions the concentration of the aqueous species  $\text{Ca}(\text{CH}_3\text{COO})_2$  increased with increasing addition of solid Ca-acetate to the solution and with increasing temperature. The solubility of  $\text{Ca}(\text{OH})_2$  in acetate solutions was investigated by Seewald et al. at high temperatures and pressures. It was found that the solubility of  $\text{Ca}(\text{OH})_2$  increased in acetate solutions. Only if the formation of  $\text{CaCH}_3\text{COO}^+$  was considered in the speciation calculations, experimental results correlated with the calculations [20–22]. Already Taylor suggested, that organic compounds could attack concrete through complexing of  $\text{Ca}^{2+}$  and consequent dissolution of  $\text{Ca}(\text{OH})_2$ , but also of hydrated silicate and aluminate phases [23]. In a study of Dramé et al. a severe leaching-dissolution effect was observed on C–S–H paste samples immersed in a Ca–Mg–acetate solution [24]. Degradation effects and altering processes on cement pastes exposed to acetate solutions were also reported in other studies [25,26].

It is well established that acetates and formates are degradable in contact with oxygen, but certain microorganisms are required to start the reactions (Eqs. (9) and (10)). A degradation mechanism could not be found in the laboratory, but in fact takes places in the field. Due to the lower oxygen demand, degradation of formates occurs faster than that of acetates. The rate of degradation increases at high temperatures, but considerably high rates are achieved even at low temperatures [27]. If the degradation products would come into contact with a saturated

solution of  $\text{Ca}(\text{OH})_2$ , poorly soluble  $\text{CaCO}_3$  will precipitate (Eq. (11)). Consequently, solid  $\text{Ca}(\text{OH})_2$  would be dissolved to maintain the equilibrium with the solution and the pH would rise (Eq. (8)). It is unknown so far, if degradation might be a significant mechanism that could affect ASR in the field, e.g. for concrete drainage systems of airports.



#### 4.2. Cement paste experiments

The cement paste experiments showed some deviating results from the solubility experiments. In fact, the K concentration increased clearly indicating the ingress of the deicing solution into the cement paste. However, the pH did not increase as much as expected and in fact decreased. Only at later ages a slight increase of the pH was observed for the low-alkali cement pastes. Generally, the pH and the Ca concentration for the samples immersed in the deicer solutions were higher than for the samples immersed in water. A problem with immersion techniques is leaching, especially for small samples with a high specific surface as it was the case in these experiments. It is suggested that among other ions cement alkalis and  $\text{OH}^-$  ions were leached from the samples at the beginning of the experiment, what finally caused the decrease of the pH. After acetate and formate ions respectively had penetrated and reacted sufficiently with  $\text{Ca}(\text{OH})_2$ , additional  $\text{OH}^-$  ions were released and the pH started to increase. Interestingly, the  $\text{SO}_4^{2-}$  concentration increased for the samples immersed in the deicer solutions, especially in the case of  $\text{HCOOK}$ . That supports the observed decomposition of ettringite by XRD analysis and the formation of the sulfur free ettringite-like phase, as often observed with ESEM/EDS [7,9,17,28,29].

#### 4.3. ASR performance tests

The concrete prisms were measured for initial length after the very first drying phase (11 days after casting) in order to cancel out the shrinkage of the prisms. The expansion after the following very first wetting and freeze–thaw–cycling (28 days after casting) is typically around 0.2 mm/m for ordinary portland cement concretes and is caused by water absorption. Only expansion beyond this hygric expansion ( $>0.2$  mm/m) is attributed to other and possibly deleterious mechanisms. For the concrete with the high-alkali portland cement ( $\text{Na}_2\text{O}_{\text{eq}} = 0.90$  wt.%), pH and alkali content in the pore solution are high enough to induce ASR even if exposed to water only. Exposed to the deicer, externally supplied K and the increasing pH highly accelerated the ASR. For both concretes with the medium- ( $\text{Na}_2\text{O}_{\text{eq}} = 0.68$  wt.%) and the low-alkali ( $\text{Na}_2\text{O}_{\text{eq}} = 0.54$  wt.%) portland cement, pH and alkali content were not sufficient to induce ASR if exposed to water only. It should be noted that the integrated freeze–thaw–cycles did not cause any frost-related damage, since no deleterious expansion occurred even after 16 cycles. This is because the mixtures were adequately air-entrained and consequently freeze–thaw resistant. However if exposed to the deicer, the medium- and even the low-alkali portland cement were not able to prevent deleterious ASR permanently. Although the expansion for the concrete with the low-alkali portland cement stays below 0.5 mm/m after 8 cycles, there is a steady increase in expansion and clear evidence for ASR was found after the cyclic climate storage in the thin section (Fig. 15) and by ESEM/EDS.

The derived mechanism helps to explain the results from the ASR performance tests of the three airfield concrete job mixtures exposed to the deicer. With decreasing  $\text{Na}_2\text{O}_{\text{eq}}$  of the cement, deleterious ASR was delayed as it took some time until sufficient amounts of K had penetrated into the concrete and until enough additional  $\text{OH}^-$  ions were released from the  $\text{Ca}(\text{OH})_2$ . Finally, all three tested concrete

mixtures are not suitable for airfield pavements where deicing/anti-icing chemicals based on acetates and formates are used. For comparison, the result for a suitable concrete mixture with sufficiently non-reactive aggregates is shown in Fig. 17.

It must be emphasized that there is no simple correlation between the number of cycles and the number of years in the field. The cyclic climate storage evaluates primarily the basic chemical and physical potentials of the concrete regarding ASR under freeze–thaw conditions, but several field specific conditions such as placing and curing, condition of the joints, influence of traffic loads etc. play a decisive role and can also affect the durability. Further studies are necessary to verify that the performance test represent the field performance of the tested concretes as was recently done for highway pavement concretes [14,15].

In addition to increased ASR, the formation of a crystal phase similar in morphology to ettringite was often observed in the near-surface zone of concretes exposed to HCOOK by ESEM/EDS [7,9,28]. However, the EDS-spectra showed that it was not ettringite due to a missing sulfur peak (Fig. 18). A former assumption that this phase may be tricarboaluminate ( $3\text{CaO} \cdot \text{Al}_2\text{O}_3 \cdot 3\text{CaCO}_3 \cdot 32\text{H}_2\text{O}$ ), the carbonate analogue of ettringite, could not be confirmed. Despite several XRD analyses, this phase could not be identified clearly. A recently conducted investigation revealed that pure synthetic ettringite was decomposed completely and altered in one or more new phases after it was stored for several days at 40 °C in a solution of HCOOK (6.0 mol/l). Whether other cement paste constituents are affected too and whether such alterations could influence the durability of concrete is unknown as of yet and these important points require further investigations.

The general findings indicate that due to the higher solubility of portlandite in the presence of acetate-based and formate-based deicers, more  $\text{OH}^-$  ions are released and consequently the pH will increase. This mechanism would clearly promote the attack of reactive aggregates (i.e. alkali-reactive silica) and could lead to accelerated ASR in concretes. This also explains why low-alkali cements are not capable of permanently preventing ASR in concretes exposed to acetate-based and formate-based deicers, if reactive aggregates are used. The alkalis from the deicers alone would not necessarily cause ASR, as long as the pH in pore solution would remain below a critical level. Since solid portlandite is also present in concretes with low-alkali cements, more and more  $\text{OH}^-$  ions will be released gradually due to the increased solubility of portlandite in contact with the deicing chemicals. Under these conditions, ASR may eventually also occur for aggregates that were assessed as moderately reactive by usual mortar bar tests (e.g. ASTM C1260, RILEM AAR-2 etc.) or concrete prism tests (e.g. ASTM C1293, RILEM AAR-3, German fog chamber method etc.).

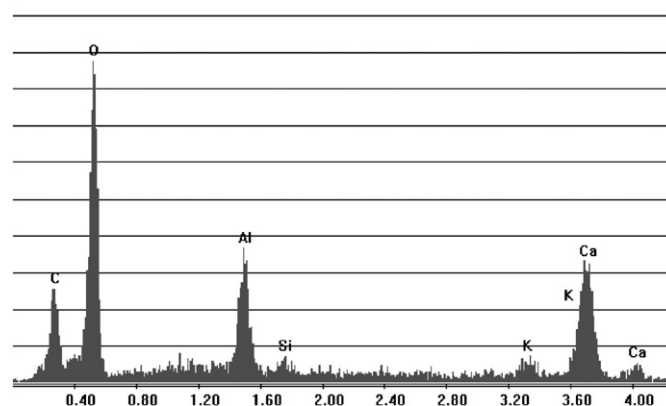
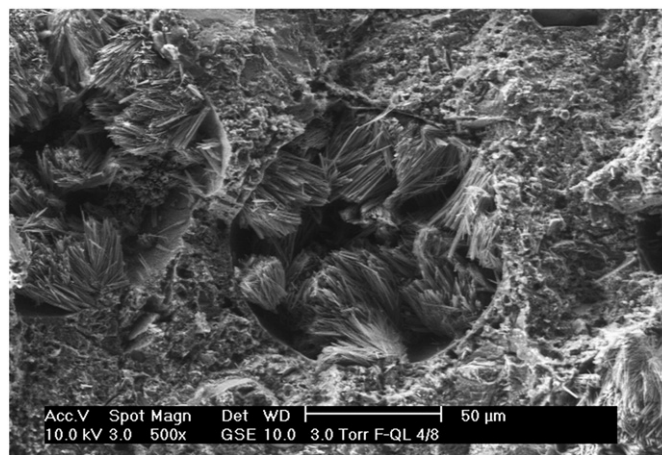


Fig. 18. Ettringite-like phase in concrete air pores (upper picture) near the concrete surface (3–5 mm) and the associated EDS-spectrum (lower picture), sample obtained from a concrete exposed to K-formate deicer solution during the cyclic climate storage.

## 5. Conclusions

Experiments on simulated pore solutions, real pore solutions and cement pastes, as well as speciation calculations and ASR performance tests were performed to explain why deicers based on acetates and formates can initiate and highly accelerate ASR in concrete with reactive and even moderately reactive aggregates. The findings from the solubility experiments showed an immediate increase of the pH and of the Ca concentration in saturated solutions of  $\text{Ca}(\text{OH})_2$  after addition of K-acetate ( $\text{CH}_3\text{COOK}$ ) and K-formate ( $\text{HCOOK}$ ) respectively, but no new reaction products were found. The speciation calculations indicate the formation of strong aqueous complexes of  $\text{CaCH}_3\text{COO}^+$ ,  $\text{Ca}(\text{CH}_3\text{COO})_2$  and  $\text{CaHCOO}^+$ ,  $\text{Ca}(\text{HCOO})_2$  respectively, resulting in an increased solubility of  $\text{Ca}(\text{OH})_2$ . Although Ca-complexes could not be found directly by any performed analysis, experiments with  $\text{CaSO}_4 \cdot 2\text{H}_2\text{O}$  support the theory of Ca-complex formation. Experiments on cement pastes showed some differing results from calculated predictions which raised additional questions, but the findings were generally supported. There is also evidence that ettringite and maybe also other cement paste constituents are altered in the presence of the deicers.

Ultimately, two chemical mechanisms seem to initiate and accelerate the ASR in concrete with reactive aggregates exposed to deicers based on acetates and formates: (1) excess supply of alkalis and (2) release of  $\text{OH}^-$  ions due to the increased solubility of  $\text{Ca}(\text{OH})_2$ . These mechanisms are able to explain the general results found by the cyclic climate storage, including the observation that low-alkali cements may delay ASR but cannot prevent it permanently in concretes with reactive and even moderately reactive aggregates which are exposed to deicers based on acetates and formates.

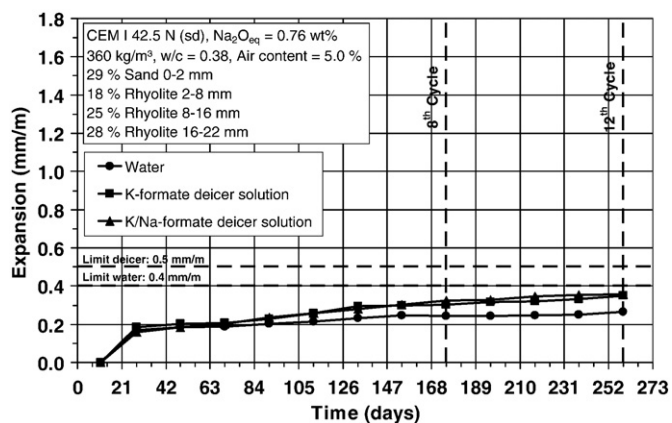


Fig. 17. Expansion during the cyclic climate storage for a tested airfield pavement concrete with non-reactive aggregates exposed to different deicer solutions and water (control).

## References

- [1] S. Chatterji, N. Thaulow, A.D. Jensen, Studies of alkali–silica reaction. Part 4. Effect of different alkali salt solutions on expansion, *Cement and Concrete Research* 17 (1987) 777–783.
- [2] M.A. Bérubé, J.F. Dorion, Laboratory and field investigations of the influence of sodium chloride on alkali–silica reactivity, alkali–aggregate reaction in concrete, *Proceedings of the 11th ICAAR, Québec City, Canada, 2000*, pp. 149–158.
- [3] L.J. Malvar, G.D. Cline, D.F. Burke, R. Rollings, T.W. Sherman, J. Greene, Alkali–Silica Reaction Mitigation: State-of-the-Art, Technical Report, Naval Facilities Engineering Service Center, 2001 TR-2195-SHR.
- [4] P.R. Rangaraju, K.R. Sompura, J. Olek, Investigation into potential of alkali-acetate-based deicers to cause alkali–silica reaction in concrete, *Journal of the Transportation Research Board* 1979 (2006) 69–78.
- [5] L.C. Martin, Alkali–Aggregate Reaction in Portland Cement Concrete (PCC) Airfield Pavements, Headquarters Air Force Civil Engineer Support Agency, Engineering Technical Letter 06-2, 2006.
- [6] P.R. Rangaraju, J. Olek, Potential for Acceleration of ASR in the Presence of Pavement Deicing Chemicals, IPRF (Innovative Pavement Research Foundation) Research Report No. 01-G-002-04-8 (2007).
- [7] J. Stark, K. Seyfarth, C. Giebson, Beurteilung der Alkali-Reaktivität von Gesteinskörnungen und AKR-Performance-Prüfung Beton, 16. Internationale Baustofftagung (ibausil), Weimar, Tagungsbericht Band 2 (2006) 399–426.
- [8] J. Stark, E. Freyburg, K. Seyfarth, C. Giebson, AKR-Prüfverfahren zur Beurteilung von Gesteinskörnungen und projektspezifischen Betonen, *beton - Die Fachzeitschrift für Bau+Technik*, Verlag Bau+Technik GmbH, Nr. 12/2006 (56. Jahrgang), pp. 574–581.
- [9] J. Stark, C. Giebson, Influence of acetate and formate based deicers on ASR in airfield concrete pavements, in: M.A.T.M. Broekmans, B.J. Wigum (Eds.), *Proceedings of the 13th ICAAR, Trondheim, Norway, 2008*, pp. 686–695.
- [10] D.L. Parkhurst, C.A.J. Appelo, PHREEQC for Windows – A computer program for speciation, batch-reaction, one-dimensional transport, and inverse geochemical calculations, Version 2.14.00 (PHREEQC-2 version 2.14.1-2217), GUI by V.E.A. Post, 2007 [http://wwwbrr.cr.usgs.gov/projects/GWC\\_coupled/phreeqc/index.html](http://wwwbrr.cr.usgs.gov/projects/GWC_coupled/phreeqc/index.html).
- [11] J. Stark, K. Seyfarth, Performance testing method for durability of concrete using climate simulation, *Proceedings of the 7th CANMET/ACI International Conference on Durability of Concrete*, Montreal, Canada, 2006, pp. 305–326.
- [12] J. Stark, C. Giebson, Assessing the durability of concrete regarding ASR, *Proceedings of the 7th CANMET/ACI International Conference on Durability of Concrete*, Montreal, Canada, 2006, pp. 225–238.
- [13] J. Stark, K. Seyfarth, Assessment of specific pavement concrete mixtures by using an ASR performance-test, in: M.A.T.M. Broekmans, B.J. Wigum (Eds.), *Proceedings of the 13th ICAAR, Trondheim, Norway, 2008*, pp. 320–329.
- [14] K. Seyfarth, C. Giebson, J. Stark, Prevention of deleterious ASR by assessing aggregates and specific concrete mixtures, *Proceedings of the 3rd International Conference on Concrete and Development*, Tehran, Iran, 2009.
- [15] K. Seyfarth, C. Giebson, J. Stark, AKR-Performance-Prüfung für Fahrbahndecken aus Beton: Erfahrungen aus Labor und Praxis im Vergleich, 17. Internationale Baustofftagung (ibausil), Weimar, Tagungsbericht Band 2 (2009) 255–260.
- [16] G. Anderson, *Thermodynamics of Natural Systems*, Second Edition, Cambridge University Press, 2005.
- [17] A. Goldbach, Einfluss von Bewegungsflächenenteisern auf die Alkali-Kieselsäure-Reaktion in Betonen für Flugbetriebsflächen, Diplomarbeit, F.A. Finger Institut für Baustoffkunde, Bauhaus-Universität Weimar, 2006.
- [18] S. Diamond, L. Kotwica, J. Olek, P.R. Rangaraju, J. Lovell, Chemical aspects of severe ASR induced by potassium acetate airfield pavement deicer solution, *Proceedings of the 8th CANMET International Conference on Recent Advances in Concrete Technology*, Marc-André Bérubé Symposium on Alkali-Aggregate Reactivity in Concrete, Montreal, Canada, 2006, pp. 261–277.
- [19] J.D. Frantz, Salts of aliphatic carboxylic acids: Raman spectra and ion pairing in hydrothermal solutions containing sodium and calcium acetates, *Chemical Geology* 164 (2000) 1–20.
- [20] S.F. Seewald, W.E. Seyfried, Experimental determination of portlandite solubility in H<sub>2</sub>O and acetate solutions at 100–350 °C and 500 bars: constraints on calcium hydroxide and calcium acetate complex stability, *Geochimica et Cosmochimica Acta* 55 (1991) 659–669.
- [21] E.L. Shock, C.M. Koretsky, Metal–organic complexes in geochemical processes: calculation of standard partial molal thermodynamic properties of aqueous acetate complexes at high pressures and temperatures, *Geochimica et Cosmochimica Acta* 57 (1993) 4899–4922.
- [22] E.L. Shock, C.M. Koretsky, Metal–organic complexes in geochemical processes: estimation of standard partial molal thermodynamic properties of aqueous complexes between metal cations and monovalent organic acid ligands at high pressures and temperatures, *Geochimica et Cosmochimica Acta* 59 (1995) 1497–1532.
- [23] H.F.W. Taylor, *Cement Chemistry*, Second Edition, Thomas Telford Publishing, London, 1997.
- [24] H. Dramé, J.J. Beaudoin, L. Raki, A comparative study of the volume stability of C–S–H (I) and portland cement paste in aqueous salt solutions, *Journal of Materials Science* 42 (16) (2007) 6837–6846.
- [25] M.C. Santagata, M. Collepardi, The effect of CMA deicers on concrete properties, *Cement and Concrete Research* 30 (2000) 1389–1394.
- [26] H. Lee, R.D. Cody, A.M. Cody, P.G. Spry, Effects of various deicing chemicals on pavement concrete deterioration, *Mid-Continent Transportation Symposium*, Center for Transportation Research and Education, Iowa State University, 2000, pp. 151–155.
- [27] K.L. Johnson, *Environmentally Safe Liquid Runway Deicer*, Cryotech Deicing Technology, Iowa, 2006.
- [28] J. Stark, F. Bellmann, B. Gathemann, K. Seyfarth, C. Giebson, The influence of alkali-containing deicing agents on the alkali–silica reaction in pavement concretes for roads and airports, *ZKG international*, No. 11–2006 (Vol. 59), pp. 74–82.
- [29] J.M. Davis, D.E. Newbury, P.R. Rangaraju, S. Soundrapanian, C. Giebson, Milli X-ray fluorescence X-ray spectrum imaging for measuring potassium ion intrusion into concrete samples, *Cement and Concrete Composites* 31 (2009) 171–175.